ELSEVIER

Inorganica Chimica Acta 225 (1994) 319–322

Inorganica Chimica Acta

Bimolecular electron transfer at high driving forces. Photoreactions of gold(I) and iridium(I) complexes with pyridinium derivatives

T. Mark McCleskey, Jay R. Winkler*, Harry B. Gray*

Beckman Institute, California Institute of Technology, Pasadena, CA 91125, USA

Received 31 March 1994

Abstract

The rates of electron transfer from electronically excited $[Au_2(1,2\text{-bis(dicyclohexylphosphino)ethane})_3]^{2+}$ (Au_2^{2+*}) and $[Ir(1,5\text{-cyclooctadiene})(\mu\text{-pyrazolyl})]_2$ (Ir_2^*) to *N*-alkylpyridinium (py^+) acceptors have been measured by Stern–Volmer quenching of Au_2^{2+*} and Ir_2^* in acetonitrile solution at 25 °C. The quenching rates increase with reaction driving force, reaching the diffusion limit at $-\Delta G° = \lambda$ and remaining at this limit for higher driving forces. The recombination reactions of pyridinyl radicals with Ir_2^+ (measured by transient absorption), however, exhibit inverted behavior at $-\Delta G°$ values greater than λ: rates decrease with increasing driving force. Formation of electronically excited products ($py^{\cdot *}/Ir_2^{+*}$) is suggested by the absence of inverted behavior for the Ir_2^*/py^+ reactions.

Keywords: Bimolecular electron transfer; Photochemistry; Gold derivatives; Iridium derivatives; Pyridinium derivatives

1. Introduction

Extensive investigations of donor–acceptor systems have shown that, at low reaction driving forces ($-\Delta G°$), electron-transfer (ET) rates (k_{ET}) increase as $-\Delta G°$ increases. As predicted by Marcus and Sutin [1], several intramolecular ET systems exhibit maximum rates at $-\Delta G° = \lambda$ (where λ is the reorganization energy for the reaction), and inverted rate/energy behavior at higher driving forces ($-\Delta G° > \lambda$) [2–10]. Interestingly, however, an inverted ET region is rarely observed in bimolecular reactions [11].

We report here on the reactions of a powerful excited-state donor, $Au_2(dcpe)_3^{2+*}$ (Au_2^{2+*}; dcpe = 1,2-bis(dicyclohexylphosphino)ethane) [12], with a series of *N*-alkylpyridinium (py^+) acceptors. In related work, we have studied ET from electronically excited $[Ir(cod)(pz)]_2$ (Ir_2^*; cod = cyclooctadiene; pz = pyrazole) to py^+ acceptors as well as the thermal recombination of pyridinyl radicals ($py^\cdot$) with $[Ir(cod)](pz)]_2^+$ (Ir_2^+) [11,13,14]. Striking differences in rate/energy behavior have been found for the Ir_2^*/py^+ and $Ir_2^+/py^\cdot$ reactions.

2. Experimental

2.1. Materials

The iridium(III) chloride was a loan from the Johnson Matthey heavy metals program. Standard methods were employed for the preparations of $[Au_2(dcpe)_3](PF_6)_2$ [12], $[Ir(cod)(pz)]_2$ [15,16] and the pyridinium hexafluorophosphates [15]. *N*-Methyl-3,4-dicyanopyridinium tetrafluoroborate was prepared according to the procedure of Burke and Brown [17]. All other chemicals were Aldrich reagent grade or better.

2.2. Lifetime and transient absorption measurements

Time-resolved luminescence and absorption measurements were performed using a conventional apparatus [18]. The excitation source was either the second ($\lambda_{ex} = 532$ nm; for Ir_2) or third ($\lambda_{ex} = 355$ nm; for Au_2^{2+}) harmonic of a Q-switched Nd:YAG laser (20 ns pulse width). All kinetics measurements were made in acetonitrile solution; the $Au_2(dcpe)_3^{2+}$ solutions were 0.1 M in Bu_4NPF_6 (Bu = n-C_4H_9) to ensure that the ionic strength remained constant.

---

*Corresponding authors.

SSDI 0020-1693(94)04063-2

2.3. Kinetics analyses

Second-order quenching rate constants were obtained from Stern–Volmer plots of excited-state decay rates versus quencher concentration. Charge-recombination rate constants were determined from non-linear least-squares fits of ΔOD versus time data ($\Delta OD_\lambda = l\Delta\epsilon C_0/(1+C_0kt)$; l = optical path length, C_0 = initial [Ir_2^+]), and from linear fits of $(\Delta OD)^{-1}$ versus time; $\Delta\epsilon_\lambda(Ir_2/Ir_2^+)$ was obtained from a transient absorption spectrum generated by quenching Ir_2^* with 380 μM methylviologen (MV^{2+}); values of $\Delta\epsilon_\lambda(MV^{\bullet+}/MV^{2+})$ are available for all wavelengths [18] and $[MV^{\bullet+}]_t$ was determined from transient absorption data at 390 nm ($\Delta\epsilon_{390}(Ir_2/Ir_2^+) \approx 0$; $\epsilon_{390}(MV^{2+}) \approx 0$; Eq. (1)).

$$\frac{\Delta OD_\lambda(t)}{\Delta OD_{390}(t)} = \frac{\Delta\epsilon_\lambda(MV^{\bullet+}/MV^{2+}) + \Delta\epsilon_\lambda(Ir_2^+/Ir_2)}{\Delta\epsilon_{390}(MV^{\bullet+}/MV^{2+})} \qquad (1)$$

3. Results and discussion

3.1. $Au_2(dcpe)_3^{2+*}/py^+$

Data for reactions between Au_2^{2+*} and a series of pyridinium cations in acetonitrile solution are set out in Table 1; the k_q values increase as the driving force increases until they reach the diffusion limit of 1.0×10^{10} $M^{-1} s^{-1}$ (Fig. 1). At very high driving forces ($-\Delta G° > 1.2$ eV), the rate constants indicate that the ET reactions are still diffusion-limited. Analysis of the Au_2^{2+*}/py^+ reactions in terms of a steady-state kinetic model (Eq. (2): k_d is the diffusion rate constant; K_d is the rate constant for formation of the donor–acceptor complex; and k_{ET} in the complex is given by Eq. (3): H_{AB} is the electronic coupling matrix element) [1,18–21] gives $\lambda = 1.66(7)$ eV and $K_d H_{AB}^2 = 110$ $M^{-1} cm^{-2}$ (vide infra). The λ value is much larger than the estimated 0.75 eV solvent contribution to the reorganization energy [18]. The extra 0.91 eV indicates that there are substantial inner-sphere changes associated with the formation of the Au(II) unit in Au_2^{3+}.

Table 1
Data for Au_2^{2+*}/py^+ ET reactions in acetonitrile solution

R_1	R_2	k_q ($M^{-1} s^{-1}$)	$-\Delta G°$ (eV)[a]
CH_3	3,4-CN	$9.5(9) \times 10^9$	2.10(5)
CH_3	4-CN	$6.7(7) \times 10^9$	1.53(5)
CH_3	$4\text{-}CO_2CH_3$	$5.1(5) \times 10^9$	1.42(5)
C_2H_5	$4\text{-}CONH_2$	$4.6(5) \times 10^9$	1.27(5)
$C_6H_5CH_2$	$3\text{-}CONH_2$	$2.1(2) \times 10^9$	1.13(5)
CH_3	$3\text{-}CONH_2$	$1.3(1) \times 10^9$	1.06(5)
C_2H_5	H	$3.7(4) \times 10^8$	0.84(5)
CH_3	$2\text{-}OCH_3$	$1.1(1) \times 10^8$	0.72(5)
CH_3	$2,3,6\text{-}CH_3$	$3.4(3) \times 10^7$	0.63(5)
CH_3	$2,4,6\text{-}CH_3$	$7.7(8) \times 10^6$	0.53(5)

[a] Corrected for work terms: Ref. [18].

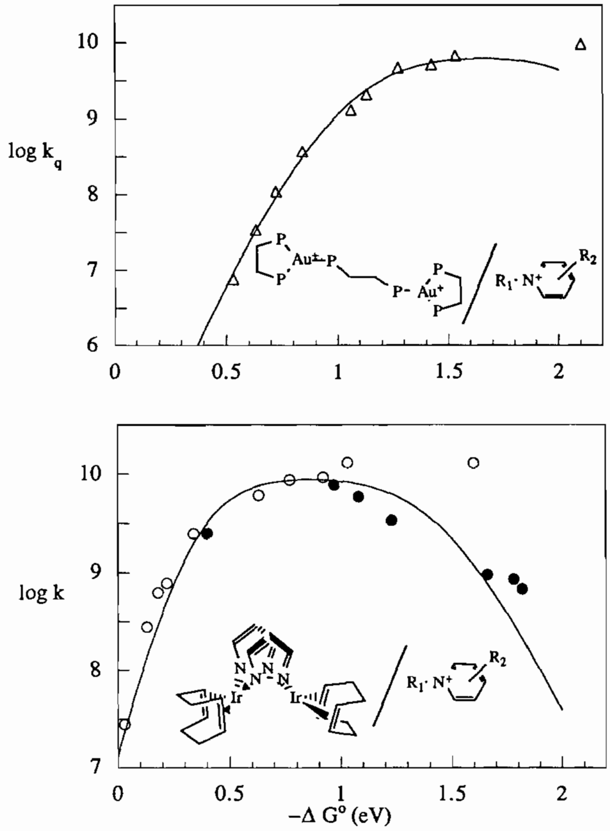

Fig. 1. Top: driving-force dependence of the ET rates from Au_2^{2+*} to py^+ quenchers in acetonitrile solution (0.1 M Bu_4NPF_6) at 25 °C. The solid curve is a fit of the data to semiclassical theory that corrects for diffusion assuming a limiting rate of 1.0×10^{10} $M^{-1} s^{-1}$. In fitting the data, the point at $-\Delta G° = 2.1$ eV was not included. Bottom: driving-force dependence of the Ir_2^*/py^+ and $Ir_2^+/py^\bullet$ ET rates in acetonitrile solution at 25 °C: (○) log k_q for the Ir_2^*/py^+ reactions; (●) log k_b for the $Ir_2^+/py^\bullet$ recombination reactions. The solid curve is a fit of the data to an ET model that includes two quantum-mechanical and one classical reorganization coordinate and corrects for diffusion assuming a limiting rate constant of 1.2×10^{10} $M^{-1} s^{-1}$ [18].

$$\frac{1}{k_q} = \frac{1}{k_d} + \frac{1}{K_d k_{ET}} \qquad (2)$$

$$k_{ET} = \frac{H_{AB}^2}{\hbar}\left[\frac{\pi}{\lambda RT}\right]^{1/2} \exp\left[\frac{-(\lambda + \Delta G°)^2}{4\lambda RT}\right] \qquad (3)$$

3.2. $[Ir(cod)(pz)]_2^*/py^+$

The lowest energy absorption band (500 nm) of Ir_2 has been assigned to a $^1[(d\sigma^*)^2] \rightarrow {}^1[(d\sigma^*)(p\sigma)]$ excitation. Luminescence at 680 nm is attributable to the corresponding $^1[(d\sigma^*)^2] \leftarrow {}^3[(d\sigma^*)(p\sigma)]$ transition; the triplet excited-state (Ir_2^*) lifetime is 240 ns in acetonitrile at room temperature [22]. The observed rate constants for ET from Ir_2^* to the py^+ acceptors increase

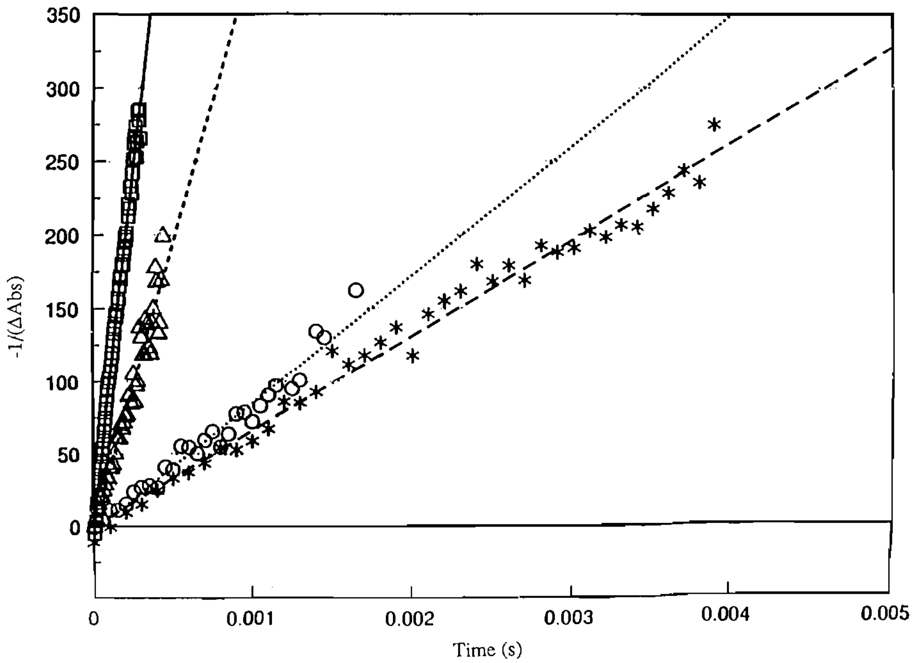

Fig. 2. Plots of $[-\Delta\mathrm{Abs}(500\ \mathrm{nm})]^{-1}$ vs. time for $Ir_2^+/py^\cdot$ recombination reactions with 4-cyano-*N*-methyl pyridinium (□), *N*-ethlylisonicotinamide (△), *N*-ethylpyridinium (○) and 2,6-dimethyl-*N*-methylpyridinium (*) in acetonitrile at 25 °C.

as the driving force increases from 0.03 to 0.92 eV, and plateau at the diffusion limit at higher driving forces (Table 2). Transient absorption measurements demonstrate that the Ir_2^*/py^+ quenching is due entirely to ET.

3.3. $[Ir(cod)(pz)]_2^+/py^\cdot$

The ET rates for charge recombination were measured by transient absorption at 500 nm ($\Delta\epsilon_{500} = -7$ $\mathrm{mM^{-1}\ cm^{-1}}$). Plots of $(\Delta OD)^{-1}$ versus time are linear with slopes $k_R/l\Delta\epsilon$ (Fig. 2). The striking feature of the data is that the rates *decrease* with increasing driving force as seen by the dramatic decrease in the slopes of the lines as the pyridinyl radicals become better donors. These recombination rates represent a rare case of inverted behavior for a series of bimolecular ET reactions.

Table 2
Data for the Ir_2^*/py^+ and $Ir_2^+/py^\cdot$ reactions in acetonitrile solution

R_1	R_2	k_q ($M^{-1}\ s^{-1}$)	$-\Delta G^\circ_q$ (eV)[a]	k_b ($M^{-1}\ s^{-1}$)	$-\Delta G^\circ_b$ (eV)[a]
CH_3	3,4-CN	$1.3(1)\times10^{10}$	1.60(5)	$2.5(3)\times10^{9}$	0.40(5)
CH_3	4-CN	$1.3(1)\times10^{10}$	1.03(5)	$7.8(8)\times10^{9}$	0.97(5)
CH_3	4-CO_2CH_3	$9.3(9)\times10^{9}$	0.92(5)	$5.9(6)\times10^{9}$	1.08(5)
C_2H_5	4-$CONH_2$	$8.8(9)\times10^{9}$	0.77(5)	$3.4(3)\times10^{9}$	1.23(5)
$C_6H_5CH_2$	3-$CONH_2$	$6.1(6)\times10^{9}$	0.63(5)	[b]	1.37(5)
C_2H_5	H	$2.5(3)\times10^{9}$	0.34(5)	$9.5(9)\times10^{8}$	1.66(5)
CH_3	2-OCH_3	$7.8(8)\times10^{8}$	0.22(5)	$8.6(9)\times10^{8}$	1.78(5)
CH_3	2,6-CH_3	$6.3(6)\times10^{8}$	0.18(5)	$6.9(7)\times10^{8}$	1.82(5)
CH_3	2,3,6-CH_3	$2.8(3)\times10^{8}$	0.13(5)	[c]	1.87(5)
CH_3	2,4,6-CH_3	$2.8(3)\times10^{7}$	0.03(5)	[c]	1.97(5)

[a] Ref. [18].

[b] Charge-recombination rate was not obtained owing to reactions of the pyridinyl radical.

[c] Transient absorption signals were below detection levels.

Although the charge-recombination rates display inverted behavior, the rates do not decrease to the extent predicted by semiclassical ET theory. An asymmetric driving-force dependence of ET rates is generally interpreted in terms of quantum-mechanical effects on nuclear reorganization [2,3,5–8]. A three-mode expression for k_{ET} (one classical mode, $\lambda_c = 0.55$ eV, and two quantum modes: $\hbar\omega_1 = 1500$, $\lambda_1 = 0.25$; $\hbar\omega_2 = 500\ \mathrm{cm^{-1}}$, $\lambda_2 = 0.05$ eV) [23] provides a good fit for the bimolecular ET rate data using Eq. (2) and the following parameters: $k_d = 1.2\times10^{10}\ M^{-1}\ s^{-1}$; $K_dH_{AB}{}^2 = 144\ M^{-1}\ cm^{-2}$ (Fig. 1). Our finding that λ (0.85 eV) is close to the values reported for intramolecular ET in two related series of Ir_2–py^+ complexes [10,24] supports the assumption that K_d remains relatively constant for the different pyridinium ions. K_d and H_{AB} cannot be separately determined from fits of driving-force data to Eqs. (2) and (3). The largest value found for H_{AB} in studies of Ir_2–py^+ intramolecular ET is 24 $\mathrm{cm^{-1}}$ [24]. This is likely to be a lower limit for the coupling in bimolecular Ir_2/py^+ ET, leading to an upper limit of $K_d < 0.25\ M^{-1}$.

The asymmetry in the driving-force dependence could also mean that the ET reactions occur over a range of distances. As the distance between donor and acceptor increases, H_{AB} decreases exponentially, but λ increases [25,26]. Since both effects lead to smaller k_{ET} values in the normal driving-force region, ET should always take place at the distance of closest approach. In the inverted driving-force region, however, the distance dependences of H_{AB} and λ on k_{ET} oppose each other; as a consequence, the optimum separation is greater than the closest approach distance. A larger reorganization energy can increase an inverted-region ($-\Delta G^\circ \sim 2$ eV) ET rate by as much as an order of magnitude [26].

The iridium–pyridinium reactions define a system where both excited-state ET and recombination rates have been observed at high driving forces. The excited-state rates plateau at the diffusion limit (Fig. 1), which is reminiscent of the findings of Rehm and Weller [27]; however, the recombination ET rates clearly show inverted behavior in the high-driving-force regime. The difference in behavior between Ir_2^*/py^+ and $Ir_2^+/py^\cdot$ rates can be explained by assuming that electronically excited products are formed in the Ir_2^*/py^+ reactions. At low driving forces, an electron will transfer exclusively from the $d\sigma^*$ orbital of Ir_2^* to the lowest π^* orbital of py^+. In the inverted region, however, fast ET can occur to yield excited products ($py^{\cdot *}/Ir_2^{+*}$) [28,29]; lowering the driving force will increase k_{ET} if the new driving force is closer to λ. Since the $Ir_2^+/py^\cdot$ reactions give products (Ir_2/py^+) in which the lowest excited state is 2.0 eV above the ground state, electronic excitation during recombination is strongly disfavored.

Acknowledgements

We thank Jim Espenson and Rudy Marcus for helpful discussions. This research was supported by National Science Foundation Grant CHE-9311587.

References

[1] R.A. Marcus and N. Sutin, *Biochim. Biophys. Acta, 811* (1985) 265.
[2] G.L. Closs, L.T. Calcaterra, N.J. Green, K.W. Penfield and J.R. Miller, *J. Phys. Chem., 90* (1986) 3673.
[3] M.R. Wasielewski, M.P. Niemcyzk, W.A. Svec and E.B. Pewitt, *J. Am. Chem. Soc., 107* (1985) 1080.
[4] G. McLendon and J.R. Miller, *J. Am. Chem. Soc., 107* (1985) 7811.
[5] I.R. Gould, D. Ege, S.L. Mattes and S. Farid, *J. Am. Chem. Soc., 109* (1987) 3794.
[6] T. Ohno, A. Yoshimura, H. Shioyama and N. Mataga, *J. Phys. Chem., 91* (1987) 4365.
[7] P.Y. Chen, R. Duesing, D.K. Graff and T.J. Meyer, *J. Phys. Chem., 95* (1991) 5850.
[8] D.B. Macqueen and K.S. Schanze, *J. Am. Chem. Soc., 113* (1991) 7470.
[9] E.H. Yonemoto, R.L. Riley, Y.I. Kim, S.J. Atherton, R.H. Schmehl and T.E. Mallouk, *J. Am. Chem. Soc., 114* (1992) 8081.
[10] L.S. Fox, M. Kozik, J.R. Winkler and H.B. Gray, *Science, 247* (1990) 1069.
[11] T.M. McCleskey, J.R. Winkler and H.B. Gray, *J. Am. Chem. Soc., 114* (1992) 6935.
[12] T.M. McCleskey and H.B. Gray, *Inorg. Chem., 31* (1992) 1733.
[13] J.L. Marshall, S.R. Stobart and H.B. Gray, *J. Am. Chem. Soc., 106* (1984) 3027.
[14] L.S. Fox, J.L. Marshall, H.B. Gray and J.R. Winkler, *J. Am. Chem. Soc., 109* (1987) 6901.
[15] J.L. Marshall, *Ph.D. Thesis*, California Institute of Technology, Pasadena, CA, 1987.
[16] G.W. Bushnell, D.O.K. Fjeldsted, S.R. Stobart, M.J. Zaworotko, S.A.R. Knox and K.A. Macpherson, *Organometallics, 4* (1985) 1107.
[17] M.R. Burke and T.L. Brown, *J. Am. Chem. Soc., 111* (1989) 5185.
[18] T.M. McCleskey, *Ph.D. Thesis,* California Institute of Technology, Pasadena, CA, 1994.
[19] C.R. Bock, J.A. Connor, A.R. Gutierrez, T.J. Meyer, D.G. Whitten, B.P. Sullivan and J.K. Nagle, *J. Am. Chem. Soc., 101* (1979) 4815.
[20] V. Balzani, L. Moggi, M.F. Manfrin and F. Bolletta, *Coord. Chem. Rev., 15* (1975) 321.
[21] N. Sutin and C. Creutz, *Pure Appl. Chem., 52* (1980) 2717.
[22] J.L. Marshall, M.D. Hopkins, V.M. Miskowski and H.B. Gray, *Inorg. Chem., 31* (1992) 5034.
[23] B.S. Brunschwig and N. Sutin, *Comments Inorg. Chem., 6* (1987) 209.
[24] R.S. Farid, I-J. Chang, J.R. Winkler and H.B. Gray, *J. Phys. Chem., 98* (1994) 5176.
[25] E.H. Yonemoto, G.P. Saupe, R.H. Schmehl, S.M. Hubig, R.L. Riley, B.L. Iverson and T.E. Mallouk, *J. Am. Chem. Soc., 116* (1994) 4786.
[26] B.S. Brunschwig, S. Ehrenson and N. Sutin, *J. Am. Chem. Soc., 106* (1984) 6858.
[27] D. Rehm and A. Weller, *Israel J. Chem., 8* (1970) 259.
[28] M. Itoh and S. Nagakura, *Bull. Chem. Soc. Jpn., 39* (1966) 369.
[29] D.L. Lichtenberger, A.S. Copenhaver, H.B. Gray, J.L. Marshall and M.D. Hopkins, *Inorg. Chem., 27* (1988) 4488.